Biochimica et Biophysica Acta 1837 (2014) 954–963

Contents lists available at ScienceDirect

Biochimica et Biophysica Acta

journal homepage: www.elsevier.com/locate/bbabio

Characterization of the type 2 NADH:menaquinone oxidoreductases from *Staphylococcus aureus* and the bactericidal action of phenothiazines ☆

Lici A. Schurig-Briccio [a], Takahiro Yano [b], Harvey Rubin [b], Robert B. Gennis [a,*]

[a] Department of Biochemistry, University of Illinois, 600 S. Mathews Street, Urbana, IL 61801, USA
[b] Department of Medicine, University of Pennsylvania, Philadelphia, PA 19104, USA

ARTICLE INFO

Article history:
Received 21 March 2014
Received in revised form 27 March 2014
Accepted 28 March 2014
Available online 5 April 2014

Keywords:
Bioenergetics/electron transfer complex
Enzyme inhibitor
Respiratory chain
Staphylococcus aureus
NADH dehydrogenase
Phenothiazine

ABSTRACT

Methicillin-resistant *Staphylococcus aureus* (MRSA) is currently one of the principal multiple drug resistant bacterial pathogens causing serious infections, many of which are life-threatening. Consequently, new therapeutic targets are required to combat such infections. In the current work, we explore the type 2 Nicotinamide adenine dinucleotide reduced form (NADH) dehydrogenases (NDH-2s) as possible drug targets and look at the effects of phenothiazines, known to inhibit NDH-2 from *Mycobacterium tuberculosis*. NDH-2s are monotopic membrane proteins that catalyze the transfer of electrons from NADH *via* flavin adenine dinucleotide (FAD) to the quinone pool. They are required for maintaining the NADH/Nicotinamide adenine dinucleotide (NAD^+) redox balance and contribute indirectly to the generation of proton motive force. NDH-2s are not present in mammals, but are the only form of respiratory NADH dehydrogenase in several pathogens, including *S. aureus*. In this work, the two putative *ndh* genes present in the *S. aureus* genome were identified, cloned and expressed, and the proteins were purified and characterized. Phenothiazines were shown to inhibit both of the *S. aureus* NDH-2s with half maximal inhibitory concentration (IC_{50}) values as low as 8 μM. However, evaluating the effects of phenothiazines on whole cells of *S. aureus* was complicated by the fact that they are also acting as uncouplers of oxidative phosphorylation. This article is part of a Special Issue entitled: 18th European Bioenergetic Conference.

1. Introduction

Persistent infections involving slow-growing or non-growing bacteria are hard to treat with antibiotics that target biosynthetic processes in growing cells [1]. Consequently, the discoveries of new drugs that disrupt membrane function (including membrane potential and energy metabolism) have been the focus of attention [2]. An example of this is the diarylquinoline TMC207, which inhibits the membrane-bound ATP synthase in *Mycobacterium tuberculosis* [3], and is the first antitubercular drug approved in 40 years (released by Johnson & Johnson). Oxidative phosphorylation is driven by the transmembrane proton motive force which is, in turn, generated by electron transfer through the respiratory chain. The respiratory enzymes of human pathogens present additional potential drug targets to disable their ability to generate energy.

Bacteria contain three distinct families of respiratory NADH:quinone oxidoreductases: Complex I, NDH-2, and a Na^+-pumping Nqr complex [4–7]. NDH-2s are composed of a single subunit of around 50 kDa with a non-covalently bound FAD as a cofactor. They are monotopic membrane proteins, being attached to the membrane through amphiphilic helices in the C-terminus [6,8]. NDH-2 catalyzes the transfer of electrons from NADH *via* FAD to membrane-bound quinone, helps to maintain the NADH/NAD^+ redox balance, and contributes indirectly to the generation of proton motive force [9]. The crystal structure of a yeast NDH-2 (Ndi1) was recently solved, demonstrating that the protein is a homodimer with an amphiphilic membrane-anchor domain [6]. Since NDH-2s are present only in bacteria and certain plant, fungal and protozoan mitochondria, but not in mammals [10–13], they are an attractive drug target and have been recognized as such for *Mycobacterium tuberculosis* [14–17], *Plasmodium falciparum* [18] and *Toxoplama gondii* [13,19]. Particularly susceptible to this drug strategy should be those pathogenic bacteria and parasites in which NDH-2 is the only respiratory NADH dehydrogenase present [13,18]. This includes *Staphylococcus aureus*.

Methicillin-resistant *S. aureus* (MRSA) is one of the principal multiple drug resistant bacterial pathogens causing serious life-threatening infections [20]. Very little is known about the biochemistry of the respiratory chain components of *S. aureus*. Analysis of the genome indicates that two types of respiratory oxygen reductases are found in *S. aureus* cells, one *bd*-type menaquinol oxidase and one heme-copper aa_3-type menaquinol oxidase. There is no bc_1 complex in *S. aureus* and no cytochrome c oxidase. L-lactate, succinate and NADH dehydrogenase activities have been detected in *S. aureus* membranes [21–25] as well as ATP synthase activity which can be inhibited by diarylquinolines related to the anti-TB drug TMC207 [26]. *S. aureus* has no Complex I (type-I

☆ This article is part of a Special Issue entitled: 18th European Bioenergetic Conference.
* Corresponding author. Tel.: +1 217 333 9075; fax: +1 217 244 3186.
E-mail address: r-gennis@illinois.edu (R.B. Gennis).

http://dx.doi.org/10.1016/j.bbabio.2014.03.017
0005-2728/

NADH:quinone oxidoreductase) but it is demonstrated in the current work that there are two functioning type-2 NADH:quinone oxidoreductases, NDH-2s, which are characterized as potential drug targets.

Phenothiazines, which are known to inhibit NDH-2 from *M. tuberculosis* and to have antitubercular activity [14,17,27], also have antibacterial activity against MRSA [28]. It is demonstrated in the current work that phenothiazines inhibit the *S. aureus* NDH-2s. However, we also show that the phenothiazines, in addition to inhibiting the respiration of *S. aureus*, are also uncouplers of oxidative phosphorylation.

2. Materials and methods

2.1. Sequence analysis

Sequences encoding NDH-2s were retrieved from the National Center for Biotechnology Information (NCBI) database. The sequences were aligned using MUSCLE [29]. Conserved residues were identified with BIOEDIT. The C-terminal amphipathic helices were predicted using PSIPRED (v3.0) [30].

2.1.1. Construction of expression plasmids

The gene encoding NdhF (SAB0804c) and NdhC (SAB0807) from *S. aureus* RF122 strain (Dr. Stefan Monecke) was cloned into pET22b (Ap^r, Novagen). To facilitate purification, an 8His-tag was introduced either in the N- or C-terminal of the *ndhF* and *ndhC* genes. The primers contained the His-tag and NdeI–HindIII restriction sites for the posterior cloning in pET22b. NdhF-Fw (5′-GGAATTCCATATGCATCACCATCACCATCACCATCACAAAAACTTAGTTTTGTTAGGCGG-3′) and NdhF-Rv (5′-CCCAAGCTTTTAACCATTATGATATTTATATAACCAAAGTACG-3′). NdhC-Fw (5′-GGAATTCCATATGGCTCAAGATCGTAAAAAAGTACT-3′) and NdhC-Rv (5′-CCCAAGCTTCTAGTGATGGTGATGGTGATGGTGGAATTTACCTTTTTGAATGCTAAAC-3′). For heterologous expression, the constructions in pET22b were transformed into *Escherichia coli* C43 (DE3) strain (Avidis, France), also containing pRARE for expression of rare codons (Km^r) [31].

2.1.2. Cell growth, enzyme expression and purification

E. coli C43 (DE3) was grown in LB medium plus 100 μg/ml ampicillin and 50 μg/ml kanamycin, at 37 °C and gene expression was induced by the addition of 1 mM IPTG (isopropyl-D-thiogalactoside) when cells reached an OD_{600} of ~0.7. All the purification procedures were carried out at 0–4 °C. Cells were harvested and resuspended in buffer A (50 mM sodium phosphate, pH 7.5, 300 mM NaCl) with 5 mM $MgSO_4$, DNAse I and a protease inhibitor cocktail (Sigma). They were then disrupted by passing twice through a microfluidizer at a pressure of 80,000 psi. Cell extract was centrifuged at 14,000 ×*g* for 10 min to remove the unbroken cells. Membranes were obtained after centrifugation at 230,000 ×*g* for 4 h. Pellets were resuspended in buffer A plus the protease inhibitor cocktail, and then solubilized by the addition of a stock solution of 20% DDM (dodecyl-β-D-maltoside) dropwise to a final concentration of 1%. The solution was incubated at 4 °C for 2 h with mild agitation. The suspension was cleared by centrifugation at 230,000 ×*g* for 1 h. The supernatant was added to Ni-NTA resin (Qiagen) pre-equilibrated with buffer A plus 0.05% DDM. The resin was washed with buffer A plus 0.05% DDM and 10–20 mM histidine and then the bound proteins were eluted with buffer A with 0.05% DDM and 100 mM histidine. Fractions were concentrated by filtration, and then the histidine was removed by dialysis against buffer A plus 0.05% DDM. The purified protein could be stored frozen at −80 °C after the addition of glycerol to a final concentration of 10%.

2.2. Analytical methods

The protein purity was evaluated by SDS-PAGE using a 4–20% gradient gel (Nusep). Protein concentration was determined using the BCA kit (Thermo Scientific, Pierce Protein Research Products). The FAD content of the isolated protein was determined spectroscopically with an Agilent Technologies spectrophotometer (model 8453), using an extinction coefficient of 11.3 cm^{-1} mM^{-1} for the free oxidized flavin at 450 nm [32], after extraction from the protein by treatment of the sample with 5% trichloroacetic acid [33].

2.3. Membrane preparations

Bacterial cells were grown in LB plus 30 mM Na-succinate for 2 or 8 h, as indicated. *E. coli* membrane preparations were carried out as described above. *S. aureus* membranes were obtained by incubating cells with lysostaphin for 2 h at 37 °C and then passing them twice through a microfluidizer at a pressure of 80,000 psi. The cell extract was centrifuged at 14,000 ×*g* for 10 min to remove the unbroken cells. Membranes were obtained by centrifugation at 230,000 ×*g* for 4 h. Pellets were resuspended in buffer A containing 10% glycerol to 30–40 mg/ml of protein and the suspension was stored at −80 °C. The respiration rates are expressed as μmol O_2 mg $protein^{-1}$ s^{-1}.

2.4. Steady state enzymatic activity assays

2.4.1. Method I: NADH dehydrogenase activity

The rate of NADH oxidation was measured at 37 °C. The 200 μl reaction mixture contained 50 mM sodium phosphate buffer, pH 7.5, 50–300 mM NaCl, 0.05% DDM, 20 μM FAD, 125 μg/ml asolectin, 0–150 μM quinone and 1–3 μg of the purified NdhF or 0.06–0.2 μg NdhC. The reaction was started with the addition of 25–250 μM NADH (prepared freshly in buffer) and the reaction's progress was monitored by the decrease in absorption of NADH at 340 nm using an Agilent 8453 UV–vis spectrophotometer. The extinction coefficient of 6.22 cm^{-1} mM^{-1} at 340 nm was used for the absorption of NADH.

2.4.2. Method II: Oxygen consumption

Oxygen concentration was monitored using a YSI model 53 oxygen electrode (Yellow Springs Instrument Co., Yellow Springs, OH) equipped with a temperature-controlled 1.8-ml electrode chamber at 37 °C. The reaction mixture for this assay consisted of sodium phosphate buffer, pH 7.5, 50–300 mM NaCl, 20 μM FAD and 200–400 μg/ml membranes and diluted isolated NdhC (0.06–0.2 μg) or NdhF (1–3 μg) enzymes. The concentration of oxygen in the air-saturated buffer at this temperature was assumed to be 250 μM, and the reaction was initiated by injecting 200 μM NADH.

2.4.3. Determination of kinetic constants

Kinetic parameters were determined using nonlinear least square analysis (Origin8.0) of the data fitted to the Michaelis–Menten rate equation ($v = V_{max}(S) / (K_m + S)$), where v is the velocity, V_{max} is the maximum velocity, S is the substrate concentration and K_m is the Michaelis–Menten constant. The enzyme rates are expressed as k_{cat}, mol NADH oxidized or mol O_2 (mol enzyme)$^{-1}$ s^{-1}. For testing inhibitors, the enzyme, in the presence of the quinone substrate (soluble analogues or membrane bound) was incubated in the reaction mix with different concentrations of the inhibitors for 3 min before NADH addition.

2.5. Membrane potential measurements

The transmembrane electrical potential (inside negative) was determined by the quenching of the potential-sensitive fluorescent probe 3,3′-dipropylthiodicarbocyanine (DisC3(5)). This lipophilic cationic dye accumulates according to the Nernst equation with high concentrations in the electrically negative phase. At high concentrations, the dye aggregates and the normal fluorescence are quenched [34,35]. Collapse of the membrane potential reverses the process and the fluorescence increases.

To perform this assay, cells of Newman strain [36] were grown for 2 h in LB and diluted to an $OD_{600\ nm}$ of 0.3 in LB plus 10 mM glucose.

Different concentrations of thioridazine (TZ) were added to the bacterial suspension as indicated. Changes in fluorescence due to the disruption of the $\Delta\psi$ were continuously monitored with a fluorescence spectrophotometer (Cary Eclipse, Agilent Technologies) employing an excitation wavelength of 643 nm and an emission wavelength of 666 nm at 30 °C. The magnitude of the $\Delta\psi$ was not quantified.

2.6. Drug susceptibility determination

The minimum inhibitory concentration (MIC) of phenothiazines on the growth of *S. aureus* was determined by starting with an overnight culture grown in LB medium, diluted to an $OD_{600\ nm}$ of 0.005, and incubated for 20 h in the presence of the drugs in microliter plates (200 μl of LB medium in 360 μl wells). The MIC reported is the lowest concentration of the phenothiazine that yields no visible growth after incubation at 37 °C, 200 rpm for 20 h.

2.7. ATP/ADP determination

S. aureus cells (Newman strain) were grown for 2 h in LB and concentrated in the same medium to an $OD_{600\ nm}$ of 2. Different concentrations of TZ, as indicated, were added and the ATP/ADP ratios were determined after 10 and 60 min of incubation at 37 °C, 200 rpm. ATP and ADP were extracted from 50 μl cell suspension by adding trichloroacetic acid (TCA) to a final concentration of 0.5%. After 5 min, TAE (Tris–acetic acid–EDTA) buffer was added to neutralize the pH by diluting the sample 5-fold. The cell content of ATP and ADP was measured according to the manufacturer's protocol (ADP/ATP Ratio Assay Kit, catalogue number: ab65313; Abcam).

2.8. Quinone extraction and analysis

The type and amount of quinone present in membranes of *E. coli* GNB10608 (MG1655 *ndh*::FRT *nuoA*::FRT) strain [37] and in the purified NDH-2s were determined by quinone extraction followed by reversed phase HPLC analysis. 10 and 30 nmol of NdhC and NdhF purified enzymes, together with 10 nmol of ubiquinone-10 (Q10) as an internal standard, were extracted with 3 ml of 6:4 methanol:petroleum ether by vortexing vigorously for 1 min (3 times). The mixture was allowed to sit for 10 min before vortexing again for an additional min, followed by centrifuging at 3000 rpm for 10 min. The pellet of 100 ml cell culture was resuspended with 3.3 ml water and extracted with 16.8 ml of 6:4 methanol:petroleum ether by vortexing vigorously for 1 min (3 times). The mixture was allowed to sit for 2 h before vortexing again for an additional min, followed by centrifuging at 3000 rpm for 10 min.

The upper organic layer was removed to a fresh flask, and the remaining mixture was subjected to further extraction two more times with 10 min incubation each. The organic phase was then evaporated under a nitrogen stream, and the dried, oily residue was re-dissolved in 4:3:3 ethanol:methanol:acetonitrile. The extracted quinones were analyzed using a reversed phase Microsorb-MV 100-5 C18 HPLC column (Varian, Palo Alto, CA) on a Beckman System Gold HPLC system fitted with a diode array detector, and monitored at 278 nm. The mobile phase was 4:3:3 ethanol:methanol:acetonitrile. The type of quinone present in the membranes was determined based on the elution of quinone standards. The amounts were calculated from the ratio of the peak areas.

2.9. Inverted membrane vesicles (IMVs)

IMVs of *E. coli* were prepared by three passages through a pre-cooled French pressure cell at 20,000 psi. The lysate was centrifuged at 14,000 ×*g* at 4 °C for 20 min to remove unbroken cells. The supernatant was centrifuged at 370,000 ×*g* at 4 °C for 1 h and the pellet consisting of the IMVs was washed with 50 mM MOPS-KOH (pH 7.5), 2 mM $MgCl_2$. After the second centrifugation step, the membranes were resuspended in 50 mM MOPS-KOH (pH 7.5), 2 mM $MgCl_2$, 10% glycerol and stored at −80 °C.

2.9.1. Assay for ATP or succinate-driven proton translocation

Proton translocation into IMVs of *E. coli* was measured by a decrease of 9-amino-6-chloro-2-methoxyacridine (ACMA) fluorescence. The excitation and emission wavelengths were 410 nm and 480 nm, respectively. IMVs (0.1 mg/ml membrane protein) were preincubated at 37 °C in 10 mM HEPES–KOH (pH 7.5), 100 mM KCl, 5 mM $MgCl_2$ containing 2 μM ACMA and the baseline was monitored for a few minutes. The reaction was then started by adding 1 mM ATP or 5 mM succinate. When the signal was stabilized, different TZ concentrations were added.

2.9.2. Determination of transmembrane $\Delta\psi$

The $\Delta\psi$-sensitive fluorophore Oxonol VI 1,5-Bis(5-oxo-3-propylisoxazol-4-yl)pentamethine oxonol was used to determine if TZ was able to dissipate the membrane potential in IMVs. *E. coli* IMVs (0.1 mg/ml membrane protein) were added to the assay buffer; 10 mM MOPS-KOH pH 7.5, 2 mM $MgCl_2$, 2 μM Oxonol VI. After a few seconds, 0.5 mM NADH was added to initiate respiration-dependent generation of $\Delta\psi$ (positive inside) and the resultant quenching of Oxonol VI fluorescence was monitored at 37 °C. The emission and excitation wavelengths were 599 nm and 634 nm, respectively. Uncoupling effect was estimated on the basis of its ability to dissipate the established $\Delta\psi$, recorded as a dequenching of the fluorescence signal.

3. Results

3.1. Sequence analysis

Inspection of the genome of the *S. aureus* RF122 strain [38] indicates the presence of genes for succinate and malate dehydrogenases, two types of menaquinol oxidases (aa_3- and *bd*-type respiratory oxygen reductases) and a nitrate reductase. There are no operons encoding for either Complex I (the energy-coupled NADH:quinone oxidoreductase) or Complex III (the quinone:cytochrome c oxidoreductase or bc_1 complex). NDH-2s have a very low sequence identity among each other, and are, therefore, difficult to reliably identify by amino acid sequence analysis alone. Enzymological characterization is always necessary. NDH-2s are characterized by the presence of (1) two GXGXXG motifs that are present at the binding sites for adenine dinucleotides [39,40]; and (2) one or two predicted amphipathic helices at the C-terminus [6,8]. Two candidate genes meet these criteria in the *S. aureus* genome and both genes are shown in this work to encode authentic NDH-2s. They will be referred to as *ndhF*, encoding the protein NdhF (NCBI gi: 3793682; SAB0804c) and *ndhC*, encoding the protein NdhC (NCBI gi: 3793685; SAB0807). NdhF and NdhC have a sequence similarity of 45%. Both NdhF and NdhC contain the two conserved GXGXXG motifs. NdhF has the first motif starting at amino acid 8 and the second motif starting at amino acid 147, and NdhC has the first motif at amino acid 12 and the second motif at amino acid 165. By using the PSIPRED (v3.0) software, one C-terminal amphipathic helix was predicted for NdhF, extended from amino acid 336 to 352 and two C-terminal amphipathic helices for NdhC, one extending from amino acid 372 to 390 and the other from amino acid 393 to398.

3.1.1. Gene expression and protein purification

The cloned *ndhF* and *ndhC* genes were expressed heterologously in *E. coli* C43(DE3). Both C- and N-terminus 8His-tag constructions were made for each, but the NdhF protein was obtained only with the N-terminal His-tag, whereas NdhC protein was obtained only with the C-terminal His-tag.

The purity and size of the isolated proteins were analyzed by SDS-PAGE (Fig. 1A). Both NdhF (Fig. 1A, lane 1) and NdhC (Fig. 1A, lane 2) run near their predicted molecular weights of ~40 kDa. The UV–visible spectra of the air-oxidized NdhF and NdhC proteins (Fig. 1B and C)

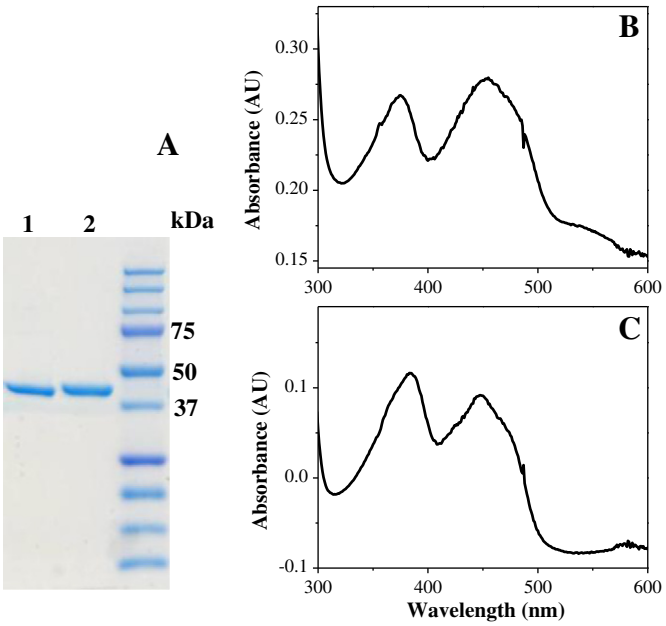

Fig. 1. SDS-PAGE and UV–visible spectra of *S. aureus* NDH-2s expressed in *E. coli*. (A) Coomassie Brilliant Blue staining of ~5 μg NdhF (lane 1) and NdhC (lane 2) proteins. (B) NdhF exhibits peaks for the oxidized FAD at 375 nm, 455 nm and 550 nm and (C) NdhC exhibits a typical UV–visible absorption spectrum of a flavoprotein, with characteristic peaks at 375 nm and 450 nm for the oxidized FAD.

show the presence of FAD, each with a peak near 450 nm and a shoulder at 465 nm indicating that the cofactor is in an apolar environment in each protein [41]. The spectrum of NdhC is typical for flavoproteins with a peak around 450 nm [42]. The spectrum NdhF at pH 7.5 shows an additional broad absorbance centered at about 550 nm (Fig. 1B). The additional absorption band results in a brick-red color of the solution of NdhF, compared to the typical yellow color of flavoproteins (including NdhC). As the solution of NdhF is made more acidic, down to pH 5, the peak at 550 nm disappears, the color changes to yellow, and the major peak shifts from 452 nm to 445 nm (Fig. S1).

Precipitation of each protein with 5% tricholoracetic acid leaves the FAD cofactor in solution, demonstrating that it is not covalently bound [43]. The amount of flavin bound to the recombinant NdhF protein was calculated to be 0.5 mol FAD/mol protein, and for NdhC was 0.25 mol FAD/mol protein. FAD loss is a common issue for flavoproteins that are heterologously expressed [44–46]. Additionally, the quinone content of NdhC and NdhF was analyzed by HPLC, and was always less than 0.03 mol quinone/mol protein.

3.2. Enzymatic characterization

The NADH:quinone oxidoreductase activities of the purified NdhF and NdhC proteins were examined with 50 μM of several soluble quinones as oxidants: menadione (MD), duroquinone (DQ), ubiquinone-1 (Q1), ubiquinone-2 (Q2), decylubiquinone (DUQ) and 2,3-dimethyl naphthoquinone (DMN) (Figs. 2 and S2). Since both proteins produced in *E. coli* have sub-stoichiometric amounts of FAD, the assays were performed in the presence of 20 μM FAD in the reaction mix. The activity of both the enzymes increased significantly when FAD as well as a lipid mixture (125 μg/ml asolectin) were added to the reaction. The increase of the specific activity corresponds roughly to full incorporation of the lost FAD cofactor. The addition of FAD or lipids separately does not increase the enzyme activity (395 ± 24 NADH s^{-1} for NdhC and 134 ± 12 NADH s^{-1} for NdhF), but when both lipids and FAD are added enzyme activity increases by an amount consistent with full incorporation of FAD into the apo-enzymes present (1500 ± 85 NADH s^{-1} for NdhC and 240 ± 17 NADH s^{-1} for NdhF). The assay buffer also contains detergent (0.05% DDM) since both NdhC and NdhF are membrane proteins. In addition, the NaCl concentration is important both for maximal protein activity and stability. NdhC is unstable at 37 °C in buffer containing less than 125 mM NaCl and in the absence of lipids. On the other hand, NdhF activity was optimal at lower concentrations of NaCl (50–100 mM) (Table 1).

The natural oxidant of both NdhF and NdhC is menaquinone in the *S. aureus* membrane [47]. In order to assay the activities of these enzymes under more native-like conditions, a protocol was devised to reconstitute the purified enzymes with *E. coli* membranes which lack endogenous NADH oxidase activity. *E. coli* membranes were isolated from a strain which lacks both NDH-2 and Complex I (Δ*ndh* Δ*nuo*) [37]. The quinone content of these membranes was determined by quinone extraction and HPLC analysis. The membranes used for these experiments were from cells grown under conditions where the major quinone present is ubiquinone-8 (Q8) (Fig. S3A). This result is consistent with previous studies [48] (Fig. S3B). NADH oxidase activity of the Δ*ndh* Δ*nuo* membranes is negligible, measured either by the oxidation of NADH or oxygen utilization. However, under the same conditions in the presence of 10 mM Na-succinate as electron donor, substantial oxygen utilization is observed (207 ± 12 μmol O_2 mg^{-1} protein s^{-1}). By the addition of a sufficient amount of *E. coli* membranes and by inclusion of FAD in the assay buffer, the maximum activities of the *S. aureus* NDH-2 enzymes were determined using Q8 as the electron acceptor. In Fig. 2, the specific activities of both enzymes are shown to be in the same range when the long chain quinone is used as the electron acceptor as when using the soluble quinone analogues. The NADH oxidation activities are increased significantly in the presence of exogenously added FAD, similar to what is observed when phospholipids are added to the assays with soluble

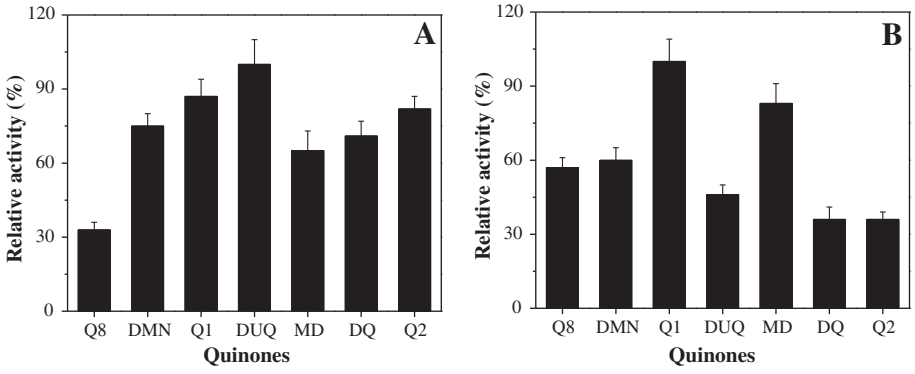

Fig. 2. Quinone-dependent enzyme activity of the *S. aureus* NDH-2s. (A) NdhF and (B) NdhC enzyme activities were measured at 37 °C with 20 μM FAD, 125 μg/ml asolectin, 50 μM different soluble quinones or 220 μg/ml *E. coli* Δ*nuo* Δ*ndh* membranes plus 100 μM NADH for NdhC and 300 μM for NdhF. Activity measured with DUQ is 320 ± 30 NADH s^{-1} (100%) for NdhF and with Q1 is 2505 ± 215 NADH s^{-1} (100%) for NdhC, and all activities are expressed as the percent relative to these values. Data are expressed as average ± SD of four independent experiments.

Table 1
Kinetic parameters of the two NDH-2s present in *S. aureus*.

	k_{cat} (NADH s^{-1})[a]	K_m NADH (μM)	K_m DMN (μM)	Preferred NaCl concentration (mM)
NdhC	1500 ± 85	35 ± 2	37.5 ± 4	125–300
NdhF	240 ± 17	154 ± 10	29.7 ± 3	50–100

Data are expressed as average ± SD of at least three independent experiments.
[a] Enzyme activity was measured at 37 °C in the presence of 125 μg/ml asolectin, 20 μM FAD, 50 μM DMN and 0.05% DDM plus 100 μM NADH for NdhC and 300 μM for NdhF, respectively.

quinone substrates. As expected, the same turnover numbers were obtained by monitoring either the oxidation of NADH spectrophotometrically or by measuring oxygen uptake using the oxygraph (corrected for 2 NADH oxidized per O_2 reduced). The data show that the isolated enzymes are competent to bind to the membrane and rapidly reduce a membrane-confined long chain quinone, and that both of the *S. aureus* NDH-2 enzymes can use either ubiquinones or menaquinones as electron acceptors.

For convenience, further steady state kinetics characterization was performed using the soluble analogue DMN (Table 1 and Fig. S2). The k_{cat} at 37 °C for the recombinant NdhF is 1500 ± 85 NADH s^{-1} and for NdhC is 240 ± 17 NADH s^{-1} (Table 1). The apparent K_m values for both NADH and DMN are in the micromolar range. NdhF has 4-fold higher K_m for NADH than NdhC, whereas the K_m for DMN is about the same for both NdhF and NdhC (Table 1). Concentrations > 250 μM NADH inhibit the activity of NdhC. Neither of the *S. aureus* NDH-2s catalyze the oxidation of NADPH and, under the conditions examined, do not directly reduce O_2 to generate reactive oxygen species.

3.3. Inhibition of the NDH-2 activity by phenothiazines

M. tuberculosis NDH-2 has been shown to be inhibited by phenothiazine [14,24]. However, the effects of phenothiazines on NDH-2s from other pathogens have not been explored. The inhibitory effects of different phenothiazine compounds on the enzyme activities of the two purified *S. aureus* NDH-2s were examined using either DMN as the electron acceptor in detergent solutions, or by coupling the enzymes to the *E. coli* respiratory chain in the absence of detergents (Tables 2 and 3). The phenothiazines were found to be more potent inhibitors when assaying the enzymes using *E. coli* membranes (Table 2), and this assay was used for most experiments (Table 3).

Three different phenothiazines were examined: TPZ, TZ and CPZ (see Table 3). Each was able to inhibit at least one of the two *S. aureus* NDH-2 enzymes, with 50% inhibition (IC_{50}) in the 10–30 μM range (Table 3). Despite the apparent similarities of these two enzymes, there must be subtle structural differences leading to differences in the way the inhibitors bind to the proteins. The best of the three inhibitors is thioridazine (TZ; see Table 3). To be certain that the NDH-2 enzymes were the actual targets of the inhibitors in the coupled assay with *E. coli* membranes, the same experiments were repeated using10 mM Na-succinate in place of NADH as the electron source and monitoring oxygen utilization. No inhibition was observed, indicating that the phenothiazines (up to 50 μM) are not inhibiting either *E. coli* succinate dehydrogenase or the *E. coli* respiratory oxygen reductases.

Table 2
Inhibition of *S. aureus* NDH-2 activity by phenothiazines.

	% of inhibition by 50 μM phenothiazines			
	NdhC		NdhF	
Quinones	TPZ	CPZ	TPZ	CPZ
Q8[a]	80 ± 10	87 ± 9	0	68 ± 7
DMN[b]	54 ± 6	73 ± 8	0	33 ± 5

Data are expressed as average ± SD of three independent experiments.
[a] Enzyme activity was measured at 37 °C in the presence of 220 μg/ml *E. coli* Δ*nuo* Δ*ndh* membranes and 20 μM FAD.
[b] Enzyme activity was measured at 37 °C in the presence of 125 μg/ml asolectin, 20 μM FAD, 50 μM DMN and 0.05% dodecylmaltoside. The substrate concentrations used were 150 μM NADH for NdhC and 300 μM for NdhF.

Table 3
IC_{50} values of phenothiazine compounds for the inhibition of NdhC and NdhF *in vitro*.

Compound	Structure	NDH-2 + Q8	IC_{50} (μM)[a]
Chlorpromazine (CPZ)	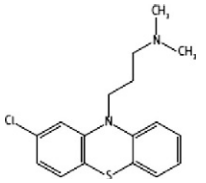	NdhC NdhF	17 ± 2.5 27.5 ± 3.5
Trifluoperazine (TPZ)	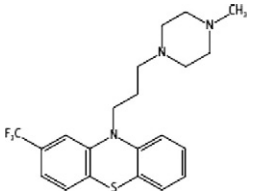	NdhC NdhF	26.5 ± 3 ≫100 μM
Thioridazine (TZ)	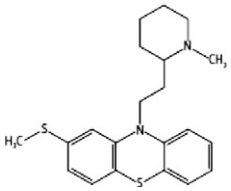	NdhC NdhF	7.9 ± 1 13.5 ± 1.5

Data are expressed as average ± SD of at least three independent experiments.
[a] Enzyme activity was measured at 37 °C in the presence of 220 μg/ml *E. coli* Δ*nuo* Δ*ndh* membranes and 20 μM FAD.

3.4. The effects of phenothiazines on S. aureus membranes

Membranes of *S. aureus* were obtained from cells grown for 14 h at 37 °C, 200 rpm. The steady-state rate of respiration of *S. aureus* membranes was determined in a cell-free amperometric assay. NADH addition to the membranes (~200 μg/ml) results in the consumption of oxygen that is fully inhibited by the addition of 50 μM of either TZ or TPZ (Table 4). The IC_{50} for *S. aureus* membranes with either drug, TZ or TPZ, is similar to those obtained with the purified NdhC protein coupled to *E. coli* respiratory chain (Tables 3 and 4). Since TPZ does not inhibit NdhF, it is concluded that when *S. aureus* is grown under these conditions, the NDH-2 present is predominantly NdhC. NADH-driven respiration of membranes is mostly inhibited by the addition of 50 μM TPZ (8 ± 1 μmol O_2 mg^{-1} protein s^{-1}), but is restored to the uninhibited activity (659 ± 28 μmol O_2 mg^{-1} protein s^{-1}) by the addition of purified NdhF (736 ± 30 μmol O_2 mg^{-1} protein s^{-1}), which reconstitutes with the *S. aureus* membranes, feeding electrons to the menaquinone pool and, from there, to the terminal oxygen reductases. The recovery of oxygen consumption implies that the site of inhibition by phenothiazines is upstream of the menaquinol-oxidases. Oxygen consumption was also examined using other electron donors: 10 mM DL-lactate, 10 mM

Table 4
Respiratory chain activity of *S. aureus* membranes and its inhibition by phenothiazines.

	Respiration activity (μmol O_2 mg^{-1} protein s^{-1})		IC_{50} (μM)	
		100 μM KCN	TPZ	TZ
NADH	659 ± 28	195 ± 10	18.5 ± 3	7.4 ± 1
DL-lactate	157 ± 15	158 ± 13	N.D.	N.D.
Na-succinate	0	N.D.	N.D.	N.D.
DL-malate	0	N.D.	N.D.	N.D.

Data are expressed as average ± SD of at least three independent experiments.
N.D.: not determined.

Na-succinate and 10 mM DL-malate. There was no detectable oxygen consumption activity with either succinate or malate, and oxidase activity with DL-lactate was about 4-fold lower than with NADH. The DL-lactate oxidase activity was not inhibited by the phenothiazines but could be 75% inhibited by 2 mM KCN (Table 4).

The fact that the respiration is not completely inhibited by 2 mM KCN suggests the presence of a cyanide-resistant cytochrome *bd* in the *S. aureus* membranes. This was confirmed spectroscopically by obtaining the NADH-reduced minus air-oxidized spectrum of *S. aureus* membranes (Fig. S4). Peaks were observed at 427 nm, 532 nm and 556 nm, which could represent both *b*-type cytochromes, 444 nm and 603 nm, corresponding to the aa_3-type oxygen reductase, and a heme *d* peak at 632 nm [49,50]. Using NADH as electron donor, oxygen consumption was inhibited 70% by the addition of 100 μM KCN. It is concluded that when grown as described, the membranes of *S. aureus* contain both the aa_3-type and *bd*-type menaquinol oxidases (Fig. S4 and Table 4).

3.5. Collapse of the membrane potential and ATP depletion

It has been established that NDH-2 indirectly contributes to the proton motive force in aerobic and hypoxic *M. tuberculosis* and that thioridazine treatment of *M. tuberculosis* causes a collapse of the membrane potential, resulting in a concomitant reduction of ATP levels as well as an increase in the intracellular NADH/NAD^+ ratio [51]. Therefore, we investigated the effects of TZ treatment of *S. aureus* cells on the membrane potential and ATP/ADP ratio (Fig. 3). Accumulation, leading to fluorescence quenching of the membrane-permeant cation DisC3(5) was used to measure the transmembrane electrical potential of intact cells in suspension. Controls to validate this method with *S. aureus* cells were performed by adding either 3 mM cyanide or 1 μM of the uncoupler CCCP to the cell suspension. Each treatment resulted in the rapid collapse of the membrane potential, indicated by an immediate increase of the DisC3(5) fluorescence intensity.

The addition of thioridazine to *S. aureus* cells also resulted in an immediate increase in DisC3(5) fluorescence, indicating collapse of the membrane potential and release of the accumulated DisC3(5). The concentration-dependence of this effect is shown in Fig. 3A. Depletion of the ATP pool followed the collapse of the proton motive force, but higher TZ concentrations and a long incubation time (60 min) were necessary to observe a significant change in the ATP/ADP ratios (Fig. 3B).

Inhibition of respiration of the cell suspension was also measured (Fig. 3C) under the same conditions used to measure the membrane potential. Surprisingly, in the presence of 50 μM TZ, which results in a rapid collapse of the membrane potential (Fig. 3A), there is virtually no inhibition of cell respiration. Inhibition of aerobic respiration in intact cells by TZ is observed only at concentrations well over 100 μM (Fig. 3C). However, when the same experiment is repeated in the presence of 1 μM CCCP, an uncoupler of oxidative phosphorylation, the addition of 50 μM TZ is sufficient to inhibit over 80% of aerobic respiration, which is completely inhibited by 100 μM TZ. This suggests that the phenothiazine TZ is being actively pumped out of *S. aureus* cells by efflux pumps, which are disabled by the presence of the protonophore CCCP. It is well established that efflux pumps are an important contributing factor to drug resistance in *S. aureus* [52]. When the efflux pumps are disabled, the intracellular concentration of TZ increases to a point where respiration by NdhC is inhibited. The data are consistent with, but do not definitively prove that NdhC is responsible for virtually all of the aerobic respiration by *S. aureus* under the growth conditions employed. Further work will be needed to further examine this.

Thioridazine is a lipophilic weak acid with a pK_a of 8.89 [53], and has been shown to be a weak uncoupler of oxidative phosphorylation with isolated rat liver mitochondria [54]. The uncoupler activity was confirmed by examining the effect of TZ on the energization of *E. coli* inverted membrane vesicles. In this system, the active site for ATP hydrolysis by the F_1F_o-ATP synthase is facing the external solution, as is the site for succinate oxidation by succinate:quinone oxidoreductase

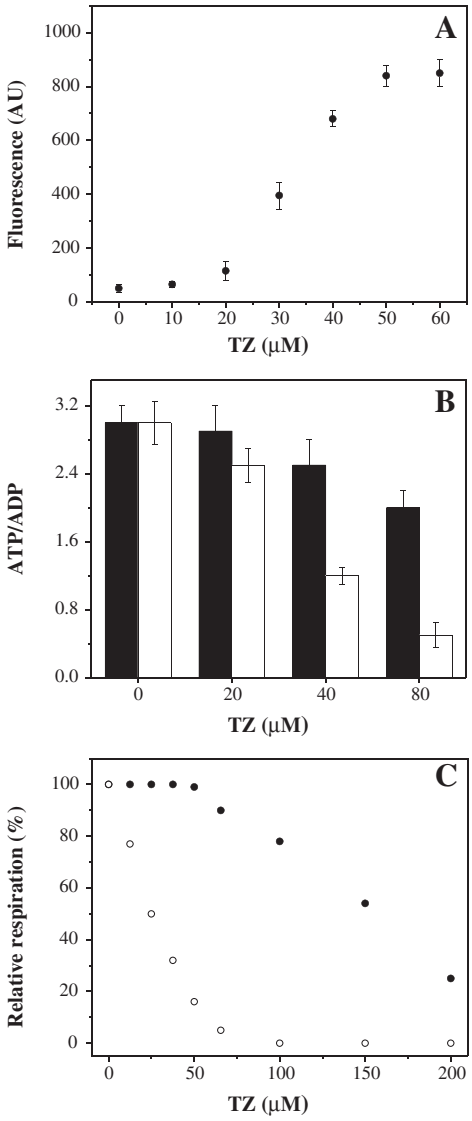

Fig. 3. Membrane potential, ATP/ADP ratios and respiration of *S. aureus* cells in the presence of TZ. (A) Fluorescence of DisC3(5) plus *S. aureus* cells immediately after the addition of different TZ concentrations as indicated (AU, arbitrary units). (B) ATP/ADP ratios of *S. aureus* cells after 10 (black bars) or 60 (white bars) min of incubation in the presence of different TZ concentrations as indicated. Data are expressed as average ± standard deviation of three independent experiments. (C) Whole cell respiration was measured in the absence (closed symbols) or presence (opened symbols) of 1 μM CCCP and different TZ concentrations as indicated. Data are representative of results of three separate experiments.

(succinate dehydrogenase/complex II). The addition of either ATP or succinate to the suspension of inverted membrane vesicles results in active proton pumping into the vesicle, corresponding to what would normally be proton pumping out of the cell. This leads to acidification of the small vesicle interior, and this acidification is monitored by the fluorescent dye ACMA (9-amino-6-chloro-2-methoxy acridine) [55] which is present in the solution. As observed in Fig. 4, the protonation of ACMA inside the acidic vesicles results in accumulation of the dye and, consequently, in fluorescence quenching [55,56]. The addition of an uncoupler (SF6847) or an inhibitor of respiration (KCN) or an inhibitor of the ATP synthase (DCCD) results in collapse of the pH gradient across the membrane and, consequently, the equilibration of the ACMA concentrations on the inside and outside of the vesicles (Fig. S5). As a result, a rapid increase of the fluorescence from ACMA, which is no longer sequestered inside the vesicles, is observed. Fig. 4 shows that 3 μM TZ is sufficient to completely collapse the pH gradient in the inverted membrane

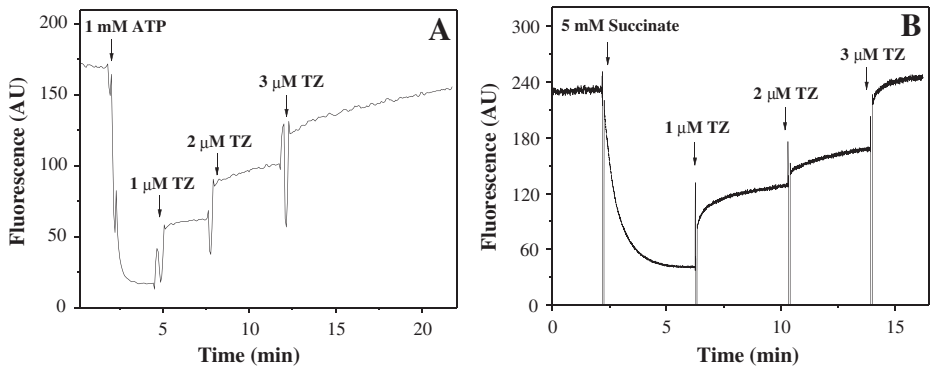

Fig. 4. Denergization of inverted membrane vesicles by TZ addition. Quenching of ACMA fluorescence in inverted membrane vesicles from *E. coli* was observed after the addition of either (A) ATP or (B) succinate. Different concentrations of the TZ compound were added after complete membrane energization. Data are representative of at least 3 independent experiments.

vesicles, whether this is generated by the ATPase or by succinate-driven respiration. As a complementary assay, $\Delta\psi$ was determined in the presence of TZ and the known uncoupler SF6847 by using the fluorescence dye Oxonol VI. Oxonol VI is an anionic slow-response probe, which exhibits potential-dependent changes in its transmembrane distribution that is accompanied by a fluorescence change [57]. Fig. 5 shows that the membrane potential is completely dissipated upon the addition of 10 μM TZ. Hence, in addition to being an inhibitor of both of the NDH-2 enzymes in *S. aureus*, TZ is also an uncoupler of oxidative phosphorylation as previously suggested [58].

4. Discussion

The current work is inspired by the recent approval of the anti-TB drug, TMC207, which inhibits the membrane-bound ATP synthase in *M. tuberculosis*, leading to the depletion of energy that is necessary for both the replicative as well as persistent states [15]. The ATP synthase is driven by the proton motive force across the cytoplasmic membrane which, in aerobic organisms, is driven by aerobic respiration. Hence, drugs targeted to the aerobic respiratory chain should be considered, particularly when pathogens have respiratory enzymes that are distinctly different from those in the mitochondrion. This is the case for the type-2 NADH dehydrogenase, or NDH-2, which is an important respiratory component in a number of pathogens but not present in the mammalian mitochondrial respiratory chain [14,16,18,19]. Indeed, NDH-2 is actively being pursued as a possible drug target against *M. tuberculosis* [14–17], *P. falciparum* [18] and *T. gondii* [13,19]. Although NDH-2 is often present in organisms that also contain alternative NADH

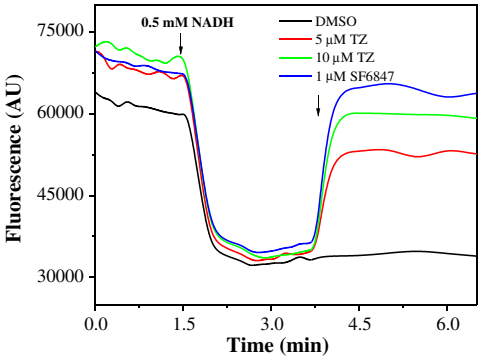

Fig. 5. Quenching of Oxonol VI fluorescence in inverted membrane vesicles in the presence of an uncoupler and TZ. Oxonol VI fluorescence in inverted membrane vesicles from *E. coli* was quenched after the addition of NADH. Upon the addition of the uncoupler SF6847 and TZ the Oxonol VI fluorescence increased due to a dissipation of the membrane potential. Data are representative of at least 3 independent experiments.

oxidizing respiratory enzymes, either Complex I or the sodium-pumping NADH:quinone oxidoreductase, in some pathogens, NDH-2 is the only respiratory NADH dehydrogenase present. This is the case for *S. aureus*, whose genome encodes two putative NDH-2s. It is very likely that the function of at least one of the NDH-2s will be essential for *S. aureus* to survive under conditions where it relies on energy production from either aerobic or anaerobic (*e.g.*, nitrate) respiration. It was recently reported that aerobic respiration is required for full *S. aureus* pathogenesis [59]. Strains of *S. aureus* that are unable to synthesize menaquinone and/or heme, although unable to respire, can survive by fermentation in a near dormant state. These respiration-impaired SCVs (small colony variants) are etiological agents of persistent infections [59]. It is not clear whether the inhibition of both NDH-2s in *S. aureus* would impact the survival of these small colony variants.

4.1. Two S. aureus NDH-2s

We have shown that each of the two genes annotated as NDH-2 in the *S. aureus* genome does encode an authentic NDH-2, denoted NdhC and NdhF. Both enzymes were produced by heterologous gene expression in *E. coli* and were shown to oxidize NADH and reduce a variety of quinones. The steady state kinetic parameters (Table 1) are different for the two enzymes though the physiological consequences are not known. Under the growth conditions employed in this work, NdhC appears to be the dominant NDH-2 present in *S. aureus* membranes, and this enzyme has a 6-fold higher k_{cat} with DMN as the electron acceptor and 4-fold lower K_M for NADH than NdhF. The k_{cat} of NdhC (1500 NADH s^{-1}) is substantially higher than those reported for NDH-2s isolated from other bacterial sources. For example, *E. coli* has an k_{cat} of ~18 NADH s^{-1} [8,10], *M. tuberculosis* of ~10 NADH s^{-1} [27], *Bacillus pseudofirmus* of ~39 NADH s^{-1} [60], *Thermus thermophilus* of ~1 NADH s^{-1} [45], *Gluconobacter oxydans* of ~9 NADH s^{-1} [61], and *Corynebacterium glutamicum* of ~213 NADH s^{-1} [62].

4.2. The red color of NdhF

Conditions under which NdhF would be present in the *S. aureus* membrane are not known. Compared to a regular flavoprotein spectrum [42], the oxidized form of purified NdhF has an unusual red color due to an absorbance band at about 550 nm. This absorbance is similar to what has been reported for flavoprotein disulfide reductases [63,64] and has been ascribed, in the AhpF protein [65], to a thiolate-FAD charge transfer band arising from the interaction with a cysteine near the C4a position of the flavin ring. This is likely also the case for NdhF, which contains 3 Cys.

4.3. A new assay for NDH-2

Because NDH-2 normally functions on the surface of a membrane bilayer using long-chain quinones as substrate, an assay was developed

to more closely mimic this situation. The purified NDH-2 enzymes from *S. aureus* are readily reconstituted with *E. coli* membranes and efficiently deliver electrons to the quinone pool, resulting in aerobic respiration. The addition of FAD to the reaction mix increases the reconstituted NADH oxidase activity, indicating that the FAD is incorporated to that portion of the recombinant protein which is purified without bound flavin thereby restoring activity. This assay avoids possible artifacts that might arise from the use of soluble quinone analogues, and can be used to better evaluate hydrophobic inhibitors. The success of this assay also implies that the two *S. aureus* NDH-2 enzymes do not require *S. aureus* phospholipids to bind to the membrane. Furthermore, this assay demonstrates that both enzymes can use long chain ubiquinone-8 (dominant in aerobically grown *E. coli*) as well as menaquinone-8 (present in *S. aureus*) as the electron acceptor. Membranes from *E. coli* were used rather than from *S. aureus* because of the availability of *E. coli* strains lacking endogenous membrane-bound NADH oxidase activity. The reconstitution also works with *S. aureus* membranes, but one needs to subtract a substantial background activity due to the presence of the NDH-2 enzymes in the membranes.

4.4. Phenothiazines inhibit both S. aureus NDH-2 enzymes

Phenothiazines are used in the clinic as neuroleptic antipsychotic drugs, but are also known to have antimicrobial activities [28,66,67]. Although they cause significant side effects, phenothiazines may offer a potential therapeutic use in problematic infections caused by antibiotic-resistant bacteria, particularly in combination with other antibiotics [68–70]. Phenothiazines inhibit *M. tuberculosis* NDH-2, which is a key enzyme in the *M. tuberculosis* respiratory chain [14,17,24,27], consistent with the transcriptional profile analysis which indicates that they act as respiratory poisons [71]. In the current work, it is shown that phenothiazines also inhibit the NDH-2 enzymes present in *S. aureus*, with the most potent being thioridazine, which inhibits both NdhC (IC_{50} = 8 μM) and NdhF (IC_{50} = 14 μM). This demonstrates that it is possible to obtain drugs that block both of these enzymes, enhancing the likelihood that drugs based on NDH-2 as a target could be therapeutically effective.

4.5. Phenothiazines are also uncouplers of oxidative phosphorylation

Although phenothiazines are effective inhibitors of the NDH-2 enzymes *in vitro*, they are not effective inhibitors with intact cells because the drugs are pumped out by efflux pumps. This is demonstrated by showing that the presence of 1 μM CCCP, a protonophore uncoupler which collapses the proton motive force, substantially increases the efficacy of thioridazine to inhibit cellular respiration (Fig. 3C). Thioridazine must be pumped out by one or more efflux pumps that are driven by the proton motive force.

Phenothiazines themselves are known to inhibit the function of some of the energy-dependent efflux pumps from *Mycobacterial* species, including *M. tuberculosis* [69,72], as well as *S. aureus* efflux pumps [52,58,73]. For this reason, phenothiazines can be used to reverse the resistance to other antibiotics [69,72]. Thioridazine (TZ; Table 3), which is less toxic to humans than chlorpromazine [74], can be used in combination with other antibiotics (*e.g.*, oxacillin) to kill MRSA as well as *M. tuberculosis* at concentrations that are tolerable in humans and can be clinically applied [58,75,76].

At least 14 efflux pumps have been described for *S. aureus* [52], and they are involved in several physiological processes, such as cell wall division, the maintenance of pH homeostasis and secretion of intracellular metabolites [77]. These pumps are driven either directly by ATP hydrolysis or by proton-flux under the control of the proton motive force [52,78,79]. The mechanism of inhibition may involve direct interactions with specific efflux pump proteins or may depend in part on reducing the magnitude of the proton motive force, and may be strain dependent [58].

The current work demonstrates that the addition of 50 μM TZ to a suspension of *S. aureus* cells, under the conditions assayed, results in the collapse of the membrane potential, which will rapidly stop from functioning any of the efflux pumps that rely directly on the proton motive force. The concentrations of phenothiazines necessary to inhibit the growth of *S. aureus* are in the same range needed to collapse the membrane potential. The reported MIC values for inhibition of growth by TZ and TPZ are 40–60 μM and that by CPZ is 90–125 μM [28,80]. The MIC values obtained in the current work are somewhat higher (Table 5) but still in the range of concentrations required for 100% collapse of the membrane potential (Fig. 3A). As previously recognized, the inactivation of efflux pumps would explain the fact that phenothiazines synergize with other antibiotics by reducing the rate at which they are being pumped out of the cell [58]. The current demonstration of the uncoupling activity of phenothiazines is also consistent with a previous report that phenothiazines act as modest uncouplers of isolated rat liver mitochondria [54]. Mitochondrial uncoupling may relate to both the therapeutic mode of action of phenothiazines as well as their toxicity.

It is paradoxical that although 50 μM TZ is sufficient to collapse the membrane potential, the intracellular concentration does not get high enough to inhibit cell respiration, whereas the presence of 1 μM CCCP allows TZ to accumulate in cells to the extent that 50 μM TZ largely eliminates cell respiration (Fig. 3). This can be explained if TZ is acting as a protonophore and the protonated, cationic form is the major current carrier across the cell membrane in response to the active proton pumps. The uncoupling mechanism requires that the neutral form of the uncoupler cross the membrane in the opposite direction (inside to outside) of the protonated form. The steady state intracellular concentration of the uncoupler will depend on the rates of the multiple kinetic steps involved. It is feasible that even under the steady state conditions where the cyclic flux of TZ is sufficient to collapse the membrane potential, the intracellular TZ concentration will not be sufficiently high to inhibit the NDH-2 enzymes. If, on the other hand, CCCP is also present, then CCCP becomes the dominant current carrier, collapsing the proton motive force, and the TZ can accumulate due to the absence of the functional efflux pumps. Whether this speculation is correct will require additional studies on the mechanism by which the phenothiazines appear to act as uncouplers.

Acknowledgments

We thank Dr. S. Monecke (Technical University of Dresden, Germany) for providing the *S. aureus* RF122 genomic DNA, Dr. H. Nikaido (University of California, Berkeley) for the pRARE2-Km plasmid, Dr. G.N. Bennett (Rice University, Houston) for the GNB10608 strain and Dr. R.K. Jayaswal (Illinois State University) for the Newman strain. We thank all the lab members for their help and useful discussions, and Dr. Ash Pawate for proofreading the text. This work was supported by grants from the National Institutes of Health, GM095600 (RBG), HL16101 (RBG) and AI068942 (HR), and the Global Alliance for TB Drug Development (HR).

Table 5
MIC for the growth of *S. aureus* by phenothiazines.

Phenothiazine	MIC (μM)
TZ	70 ± 9
TPZ	70 ± 10
CPZ	170 ± 15

Data are expressed as average ± SD of four independent experiments. The MIC is the lowest concentration of the compound required to eliminate visible growth in liquid culture under conditions described in the text.

Appendix A. Supplementary data

Supplementary data to this article can be found online at http://dx.doi.org/10.1016/j.bbabio.2014.03.017.

References

[1] I. Chopra, L. Hesse, A.J. O'Neill, Exploiting current understanding of antibiotic action for discovery of new drugs, Symp. Ser. Soc. Appl. Microbiol. (2002) 4S–15S.
[2] J.G. Hurdle, A.J. O'Neill, I. Chopra, R.E. Lee, Targeting bacterial membrane function: an underexploited mechanism for treating persistent infections, Nat. Rev. Microbiol. 9 (2011) 62–75.
[3] K. Andries, P. Verhasselt, J. Guillemont, H.W. Gohlmann, J.M. Neefs, H. Winkler, J. Van Gestel, P. Timmerman, M. Zhu, E. Lee, P. Williams, D. de Chaffoy, E. Huitric, S. Hoffner, E. Cambau, C. Truffot-Pernot, N. Lounis, V. Jarlier, A diarylquinoline drug active on the ATP synthase of *Mycobacterium tuberculosis*, Science 307 (2005) 223–227.
[4] H. Angerer, H.R. Nasiri, V. Niedergesass, S. Kerscher, H. Schwalbe, U. Brandt, Tracing the tail of ubiquinone in mitochondrial complex I, Biochim. Biophys. Acta 1817 (2012) 1776–1784.
[5] R.G. Efremov, L.A. Sazanov, Structure of the membrane domain of respiratory complex I, Nature 476 (2011) 414–420.
[6] Y. Feng, W. Li, J. Li, J. Wang, J. Ge, D. Xu, Y. Liu, K. Wu, Q. Zeng, J.W. Wu, C. Tian, B. Zhou, M. Yang, Structural insight into the type-II mitochondrial NADH dehydrogenases, Nature 491 (2012) 478–482.
[7] O. Juarez, B. Barquera, Insights into the mechanism of electron transfer and sodium translocation of the Na(+)-pumping NADH:quinone oxidoreductase, Biochim. Biophys. Acta 1817 (2012) 1823–1832.
[8] J.M. Villegas, S.I. Volentini, M.R. Rintoul, V.A. Rapisarda, Amphipathic C-terminal region of *Escherichia coli* NADH dehydrogenase-2 mediates membrane localization, Arch. Biochem. Biophys. 505 (2011) 155–159.
[9] S. Kerscher, S. Drose, V. Zickermann, U. Brandt, The three families of respiratory NADH dehydrogenases, Results Probl. Cell Differ. 45 (2008) 185–222.
[10] A. Jaworowski, G. Mayo, D.C. Shaw, H.D. Campbell, I.G. Young, Characterization of the respiratory NADH dehydrogenase of *Escherichia coli* and reconstitution of NADH oxidase in ndh mutant membrane vesicles, Biochemistry 20 (1981) 3621–3628.
[11] A.M. Melo, M. Duarte, A. Videira, Primary structure and characterisation of a 64 kDa NADH dehydrogenase from the inner membrane of *Neurospora crassa* mitochondria, Biochim. Biophys. Acta 1412 (1999) 282–287.
[12] A.G. Rasmusson, A.S. Svensson, V. Knoop, L. Grohmann, A. Brennicke, Homologues of yeast and bacterial rotenone-insensitive NADH dehydrogenases in higher eukaryotes: two enzymes are present in potato mitochondria, Plant J. 20 (1999) 79–87.
[13] S.S. Lin, U. Gross, W. Bohne, Type II NADH dehydrogenase inhibitor 1-hydroxy-2-dodecyl-4(1H)quinolone leads to collapse of mitochondrial inner-membrane potential and ATP depletion in *Toxoplasma gondii*, Eukaryot. Cell 8 (2009) 877–887.
[14] A.J. Warman, T.S. Rito, N.E. Fisher, D.M. Moss, N.G. Berry, P.M. O'Neill, S.A. Ward, G.A. Biagini, Antitubercular pharmacodynamics of phenothiazines, J. Antimicrob. Chemother. 68 (2013) 869–880.
[15] D. Bald, A. Koul, Respiratory ATP synthesis: the new generation of mycobacterial drug targets? FEMS Microbiol. Lett. 308 (2010) 1–7.
[16] P.S. Shirude, B. Paul, N. Roy Choudhury, C. Kedari, B. Bandodkar, B.G. Ugarkar, Quinolinyl pyrimidines: potent inhibitors of NDH-2 as a novel class of anti-TB agents, ACS Med. Chem. Lett. 3 (2012) 736–740.
[17] E.A. Weinstein, T. Yano, L.S. Li, D. Avarbock, A. Avarbock, D. Helm, A.A. McColm, K. Duncan, J.T. Lonsdale, H. Rubin, Inhibitors of type II NADH:menaquinone oxidoreductase represent a class of antitubercular drugs, Proc. Natl. Acad. Sci. U. S. A. 102 (2005) 4548–4553.
[18] G.A. Biagini, N. Fisher, A.E. Shone, M.A. Mubaraki, A. Srivastava, A. Hill, T. Antoine, A.J. Warman, J. Davies, C. Pidathala, R.K. Amewu, S.C. Leung, R. Sharma, P. Gibbons, D.W. Hong, B. Pacorel, A.S. Lawrenson, S. Charoensutthivarakul, L. Taylor, O. Berger, A. Mbekeani, P.A. Stocks, G.L. Nixon, J. Chadwick, J. Hemingway, M.J. Delves, R.E. Sinden, A.M. Zeeman, C.H. Kocken, N.G. Berry, P.M. O'Neill, S.A. Ward, Generation of quinolone antimalarials targeting the *Plasmodium falciparum* mitochondrial respiratory chain for the treatment and prophylaxis of malaria, Proc. Natl. Acad. Sci. U. S. A. 109 (2012) 8298–8303.
[19] S.S. Lin, U. Gross, W. Bohne, Two internal type II NADH dehydrogenases of *Toxoplasma gondii* are both required for optimal tachyzoite growth, Mol. Microbiol. 82 (2011) 209–221.
[20] M.A. Fischbach, C.T. Walsh, Antibiotics for emerging pathogens, Science 325 (2009) 1089–1093.
[21] V. Artzatbanov, V.V. Petrov, Branched respiratory chain in aerobically grown *Staphylococcus aureus*—oxidation of ethanol by cells and protoplasts, Arch. Microbiol. 153 (1990) 580–584.
[22] A. Sasarman, P. Purvis, V. Portelance, Role of menaquinone in nitrate respiration in *Staphylococcus aureus*, J. Bacteriol. 117 (1974) 911–913.
[23] Z. Tynecka, Z. Szczesniak, A. Malm, R. Los, Energy conservation in aerobically grown *Staphylococcus aureus*, Res. Microbiol. 150 (1999) 555–566.
[24] T. Yano, S. Kassovska-Bratinova, J.S. Teh, J. Winkler, K. Sullivan, A. Isaacs, N.M. Schechter, H. Rubin, Reduction of clofazimine by mycobacterial type 2 NADH: quinone oxidoreductase: a pathway for the generation of bactericidal levels of reactive oxygen species, J. Biol. Chem. 286 (2011) 10276–10287.
[25] J.R. Fuller, N.P. Vitko, E.F. Perkowski, E. Scott, D. Khatri, J.S. Spontak, L.R. Thurlow, A.R. Richardson, Identification of a lactate-quinone oxidoreductase in *Staphylococcus aureus* that is essential for virulence, Front. Cell. Infect. Microbiol. 1 (2011) 19.
[26] W. Balemans, L. Vranckx, N. Lounis, O. Pop, J. Guillemont, K. Vergauwen, S. Mol, R. Gilissen, M. Motte, D. Lancois, M. De Bolle, K. Bonroy, H. Lill, K. Andries, D. Bald, A. Koul, Novel antibiotics targeting respiratory ATP synthesis in Gram-positive pathogenic bacteria, Antimicrob. Agents Chemother. 56 (2012) 4131–4139.
[27] T. Yano, L.S. Li, E. Weinstein, J.S. Teh, H. Rubin, Steady-state kinetics and inhibitory action of antitubercular phenothiazines on *Mycobacterium tuberculosis* type-II NADH-menaquinone oxidoreductase (NDH-2), J. Biol. Chem. 281 (2006) 11456–11463.
[28] D. Ordway, M. Viveiros, C. Leandro, M.J. Arroz, L. Amaral, Intracellular activity of clinical concentrations of phenothiazines including thioridiazine against phagocytosed *Staphylococcus aureus*, Int. J. Antimicrob. Agents 20 (2002) 34–43.
[29] R.C. Edgar, MUSCLE: a multiple sequence alignment method with reduced time and space complexity, BMC Bioinforma. 5 (2004) 113.
[30] D.T. Jones, Protein secondary structure prediction based on position-specific scoring matrices, J. Mol. Biol. 292 (1999) 195–202.
[31] H.S. Kim, D. Nagore, H. Nikaido, Multidrug efflux pump MdtBC of *Escherichia coli* is active only as a B2C heterotrimer, J. Bacteriol. 192 (2010) 1377–1386.
[32] A. Aliverti, B. Curti, M.A. Vanoni, Identifying and quantitating FAD and FMN in simple and in iron–sulfur-containing flavoproteins, Methods Mol. Biol. 131 (1999) 9–23.
[33] S. Susin, J. Abian, F. Sanchez-Baeza, M.L. Peleato, A. Abadia, E. Gelpi, J. Abadia, Riboflavin 3′- and 5′-sulfate, two novel flavins accumulating in the roots of iron-deficient sugar beet (*Beta vulgaris*), J. Biol. Chem. 268 (1993) 20958–20965.
[34] M. Wu, R.E. Hancock, Interaction of the cyclic antimicrobial cationic peptide bactenecin with the outer and cytoplasmic membrane, J. Biol. Chem. 274 (1999) 29–35.
[35] R.J. Brooijmans, B. Poolman, G.K. Schuurman-Wolters, W.M. de Vos, J. Hugenholtz, Generation of a membrane potential by *Lactococcus lactis* through aerobic electron transport, J. Bacteriol. 189 (2007) 5203–5209.
[36] E.S. Duthie, L.L. Lorenz, Staphylococcal coagulase; mode of action and antigenicity, J. Gen. Microbiol. 6 (1952) 95–107.
[37] N.R. Yun, K.Y. San, G.N. Bennett, Enhancement of lactate and succinate formation in adhE or pta-ackA mutants of NADH dehydrogenase-deficient *Escherichia coli*, J. Appl. Microbiol. 99 (2005) 1404–1412.
[38] L. Herron-Olson, J.R. Fitzgerald, J.M. Musser, V. Kapur, Molecular correlates of host specialization in *Staphylococcus aureus*, PLoS One 2 (2007) e1120.
[39] M.G. Rossmann, D. Moras, K.W. Olsen, Chemical and biological evolution of nucleotide-binding protein, Nature 250 (1974) 194–199.
[40] C.R. Bellamacina, The nicotinamide dinucleotide binding motif: a comparison of nucleotide binding proteins, FASEB J. 10 (1996) 1257–1269.
[41] S. Ghisla, V. Massey, New flavins for old: artificial flavins as active site probes of flavoproteins, Biochem. J. 239 (1986) 1–12.
[42] S. Ghisla, V. Massey, J.M. Lhoste, S.G. Mayhew, Fluorescence and optical characteristics of reduced flavines and flavoproteins, Biochemistry 13 (1974) 589–597.
[43] N.S. Scrutton, Identification of covalent flavoproteins and analysis of the covalent link, Methods Mol. Biol. 131 (1999) 181–193.
[44] C. Griesbeck, M. Schutz, T. Schodl, S. Bathe, L. Nausch, N. Mederer, M. Vielreicher, G. Hauska, Mechanism of sulfide-quinone reductase investigated using site-directed mutagenesis and sulfur analysis, Biochemistry 41 (2002) 11552–11565.
[45] P. Venkatakrishnan, A.M. Lencina, L.A. Schurig-Briccio, R.B. Gennis, Alternate pathways for NADH oxidation in *Thermus thermophilus* using type 2 NADH dehydrogenases, Biol. Chem. 394 (2013) 667–676.
[46] A.M. Lencina, Z. Ding, L.A. Schurig-Briccio, R.B. Gennis, Characterization of the Type III sulfide:quinone oxidoreductase from *Caldivirga maquilingensis* and its membrane binding, Biochim. Biophys. Acta 1827 (2012) 266–275.
[47] R. Bentley, R. Meganathan, Biosynthesis of vitamin K (menaquinone) in bacteria, Microbiol. Rev. 46 (1982) 241–280.
[48] M. Bekker, G. Kramer, A.F. Hartog, M.J. Wagner, C.G. de Koster, K.J. Hellingwerf, M.J. de Mattos, Changes in the redox state and composition of the quinone pool of *Escherichia coli* during aerobic batch-culture growth, Microbiology 153 (2007) 1974–1980.
[49] R.M. Lorence, J.G. Koland, R.B. Gennis, Coulometric and spectroscopic analysis of the purified cytochrome d complex of *Escherichia coli*: evidence for the identification of "cytochrome a1" as cytochrome b595, Biochemistry 25 (1986) 2314–2321.
[50] C.W. Jones, R.K. Poole, 10 The analysis of cytochromes, in: T. Bergan (Ed.), Methods in Microbiology, Academic Press, 1985, pp. 285–328.
[51] S.P. Rao, S. Alonso, L. Rand, T. Dick, K. Pethe, The protonmotive force is required for maintaining ATP homeostasis and viability of hypoxic, nonreplicating *Mycobacterium tuberculosis*, Proc. Natl. Acad. Sci. U. S. A. 105 (2008) 11945–11950.
[52] S.S. Costa, M. Viveiros, L. Amaral, I. Couto, Multidrug efflux pumps in *Staphylococcus aureus*: an update, Open Microbiol. J. 7 (2013) 59–71.
[53] U. Domanska, A. Pobudkowska, A. Pelczarska, Solubility of sparingly soluble drug derivatives of anthranilic acid, J. Phys. Chem. B 115 (2011) 2547–2554.
[54] J.S. Modica-Napolitano, C.J. Lagace, W.A. Brennan, J.R. Aprille, Differential effects of typical and atypical neuroleptics on mitochondrial function in vitro, Arch. Pharm. Res. 26 (2003) 951–959.
[55] J. Han, K. Burgess, Fluorescent indicators for intracellular pH, Chem. Rev. 110 (2010) 2709–2728.
[56] J.P. Dufour, A. Goffeau, T.Y. Tsong, Active proton uptake in lipid vesicles reconstituted with the purified yeast plasma membrane ATPase. Fluorescence quenching of 9-amino-6-chloro-2-methoxyacridine, J. Biol. Chem. 257 (1982) 9365–9371.
[57] H.J. Apell, B. Bersch, Oxonol VI as an optical indicator for membrane potentials in lipid vesicles, Biochim. Biophys. Acta 903 (1987) 480–494.
[58] G.W. Kaatz, V.V. Moudgal, S.M. Seo, J.E. Kristiansen, Phenothiazines and thioxanthenes inhibit multidrug efflux pump activity in *Staphylococcus aureus*, Antimicrob. Agents Chemother. 47 (2003) 719–726.
[59] N.D. Hammer, M.L. Reniere, J.E. Cassat, Y. Zhang, A.O. Hirsch, M. Indriati Hood, E.P. Skaar, Two heme-dependent terminal oxidases power *Staphylococcus aureus* organ-specific colonization of the vertebrate host, MBio 4 (2013).

[60] J. Liu, T.A. Krulwich, D.B. Hicks, Purification of two putative type II NADH dehydrogenases with different substrate specificities from alkaliphilic *Bacillus pseudofirmus* OF4, Biochim. Biophys. Acta (BBA) Bioenerg. 1777 (2008) 453–461.
[61] T. Mogi, K. Matsushita, Y. Murase, K. Kawahara, H. Miyoshi, H. Ui, K. Shiomi, S. Omura, K. Kita, Identification of new inhibitors for alternative NADH dehydrogenase (NDH-II), FEMS Microbiol. Lett. 291 (2009) 157–161.
[62] N. Nantapong, A. Otofuji, C.T. Migita, O. Adachi, H. Toyama, K. Matsushita, Electron transfer ability from NADH to menaquinone and from NADPH to oxygen of type II NADH dehydrogenase of *Corynebacterium glutamicum*, Biosci. Biotechnol. Biochem. 69 (2005) 149–159.
[63] A.J. Prongay, D.R. Engelke, C.H. Williams Jr., Characterization of two active site mutations of thioredoxin reductase from *Escherichia coli*, J. Biol. Chem. 264 (1989) 2656–2664.
[64] A.J. Prongay, C.H. Williams Jr., Oxidation–reduction properties of *Escherichia coli* thioredoxin reductase altered at each active site cysteine residue, J. Biol. Chem. 267 (1992) 25181–25188.
[65] T.J. Jonsson, H.R. Ellis, L.B. Poole, Cysteine reactivity and thiol-disulfide interchange pathways in AhpF and AhpC of the bacterial alkyl hydroperoxide reductase system, Biochemistry 46 (2007) 5709–5721.
[66] L. Amaral, M. Viveiros, J. Molnar, Antimicrobial activity of phenothiazines, In Vivo 18 (2004) 725–731.
[67] D. Takacs, P. Cerca, A. Martins, Z. Riedl, G. Hajos, J. Molnar, M. Viveiros, I. Couto, L. Amaral, Evaluation of forty new phenothiazine derivatives for activity against intrinsic efflux pump systems of reference *Escherichia coli*, *Salmonella* Enteritidis, *Enterococcus faecalis* and *Staphylococcus aureus* strains, In Vivo 25 (2011) 719–724.
[68] A.T. Fafarman, P.A. Sigala, J.P. Schwans, T.D. Fenn, D. Herschlag, S.G. Boxer, Quantitative, directional measurement of electric field heterogeneity in the active site of ketosteroid isomerase, Proc. Natl. Acad. Sci. U. S. A. 109 (2012) E299–308.
[69] L. Amaral, J. Molnar, Why and how the old neuroleptic thioridazine cures the XDR-TB patient, Pharmaceuticals (Basel) 5 (2012) 1021–1031.
[70] L. Amaral, Z. Udwadia, E. Abbate, D. van Soolingen, The added effect of thioridazine in the treatment of drug-resistant tuberculosis, Int. J. Tuberc. Lung Dis. 16 (2012) 1706–1708 (author reply 1708–1709).
[71] P.A. Mak, S.P. Rao, M. Ping Tan, X. Lin, J. Chyba, J. Tay, S.H. Ng, B.H. Tan, J. Cherian, J. Duraiswamy, P. Bifani, V. Lim, B.H. Lee, N. Ling Ma, D. Beer, P. Thayalan, K. Kuhen, A. Chatterjee, F. Supek, R. Glynne, J. Zheng, H.I. Boshoff, C.E. Barry 3rd, T. Dick, K. Pethe, L.R. Camacho, A high-throughput screen to identify inhibitors of ATP homeostasis in non-replicating *Mycobacterium tuberculosis*, ACS Chem. Biol. 7 (2012) 1190–1197.
[72] L. Rodrigues, D. Wagner, M. Viveiros, D. Sampaio, I. Couto, M. Vavra, W.V. Kern, L. Amaral, Thioridazine and chlorpromazine inhibition of ethidium bromide efflux in *Mycobacterium avium* and *Mycobacterium smegmatis*, J. Antimicrob. Chemother. 61 (2008) 1076–1082.
[73] M.M. Kristiansen, C. Leandro, D. Ordway, M. Martins, M. Viveiros, T. Pacheco, J. Molnar, J.E. Kristiansen, L. Amaral, Thioridazine reduces resistance of methicillin-resistant *Staphylococcus aureus* by inhibiting a reserpine-sensitive efflux pump, In Vivo 20 (2006) 361–366.
[74] J. Hyttel, J.J. Larsen, A.V. Christensen, J. Arnt, Receptor-binding profiles of neuroleptics, Psychopharmacology Suppl. 2 (1985) 9–18.
[75] M. Martins, W. Bleiss, A. Marko, D. Ordway, M. Viveiros, C. Leandro, T. Pacheco, J. Molnar, J.E. Kristiansen, L. Amaral, Clinical concentrations of thioridazine enhance the killing of intracellular methicillin-resistant *Staphylococcus aureus*: an in vivo, ex vivo and electron microscopy study, In Vivo 18 (2004) 787–794.
[76] R.H. Thanacoody, Thioridazine: the good and the bad, Recent Pat. Antiinfect. Drug Discov. 6 (2011) 92–98.
[77] L.J. Piddock, Multidrug-resistance efflux pumps — not just for resistance, Nat. Rev. Microbiol. 4 (2006) 629–636.
[78] P. Mazurkiewicz, G.J. Poelarends, A.J. Driessen, W.N. Konings, Facilitated drug influx by an energy-uncoupled secondary multidrug transporter, J. Biol. Chem. 279 (2004) 103–108.
[79] X.Z. Li, H. Nikaido, Efflux-mediated drug resistance in bacteria: an update, Drugs 69 (2009) 1555–1623.
[80] O. Hendricks, T.S. Butterworth, J.E. Kristiansen, The in-vitro antimicrobial effect of non-antibiotics and putative inhibitors of efflux pumps on *Pseudomonas aeruginosa* and *Staphylococcus aureus*, Int. J. Antimicrob. Agents 22 (2003) 262–264.